Eur. Phys. J. B **62**, 341–348 (2008)
DOI: 10.1140/epjb/e2008-00154-5

THE EUROPEAN PHYSICAL JOURNAL B

Study of transients in the propagation of nonlinear waves in some reaction diffusion systems

L. Giuggioli[a], Z. Kalay, and V.M. Kenkre

Consortium of the Americas for Interdisciplinary Science and Department of Physics and Astronomy, University of New Mexico, Albuquerque, New Mexico 87131, USA

Received 14 June 2007 / Received in final form 2 March 2008
Published online 11 April 2008 –

Abstract. We study the transient dynamics of single species reaction diffusion systems whose reaction terms $f(u)$ vary nonlinearly near $u \approx 0$, specifically as $f(u) \approx u^2$ and $f(u) \approx u^3$. We consider three cases, calculate their traveling wave fronts and speeds *analytically* and solve the equations numerically with different initial conditions to study the approach to the asymptotic front shape and speed. Observed time evolution is found to be quite sensitive to initial conditions and to display in some cases nonmonotonic behavior, ascribable to the disparity in time scales between the evolution of the front interior and the front tail.

PACS. 82.40.Ck Pattern formation in reactions with diffusion, flow and heat transfer – 47.20.Ky Nonlinearity, bifurcation, and symmetry breaking – 05.45.-a Nonlinear dynamics and chaos

1 Introduction

Reaction diffusion models are ubiquitous in science. They are commonly employed to represent systems whose components move diffusively and whose interaction events, described by the reaction terms, may be represented by nonlinear expressions in the macroscopic observables such as the system density. Common examples can be found in aggregation [1], deposition [2], chemical reactions [3], flame combustion [4], pulse propagation in nerves [5] and population dynamics [6,7]. Extensions of reaction diffusion studies to convective transport [8,9], non-diffusive transport [10,11] and spatially non-local interactions [12,13] have also been studied in the recent past. Here we restrict our attention to a single-species reaction diffusion equation in 1-D in its simplest form, i.e.,

$$\frac{\partial u(x,t)}{\partial t} = D\frac{\partial^2 u(x,t)}{\partial x^2} + af(u), \tag{1}$$

where $u(x,t)$ represents the density profile of the species expressed here as a dimensionless quantity, D is the diffusion constant, a the growth rate and $f(u)$ the nonlinearity. We will further assume that $f(0) = f(1) = 0$, which is a property of the nonlinearity in many systems of interest.

Equations such as (1) often result in propagating wavefronts. The class of reaction terms that allows this feature is rather broad but three generic types of nonlinearity may be distinguished [14]. One type, henceforth called the *first type*, corresponds to positive $f(u)$ for $0 < u < 1$ with $f(u) \approx u$ for $u \approx 0$. A well-known example is provided by the Fisher-Kolmogorov-Petrovskii-Piskunov (FKPP) equation [15,16] whose reaction term is $f(u) = u(1-u)$. Another type, henceforth called the *second type*, corresponds to negative $f(u)$ for $0 < u < b$ and positive $f(u)$ for $b < u < 1$ such as the Zel'dovich—Frank-Kamenetsky [17] equation (ZF), also referred to in the literature as the reduced Nagumo equation [7], for which $f(u) = u(u-b)(1-u)$ with $0 < b < 1$. This change of sign in the nonlinearity is responsible to what is referred to in population dynamics as the Allee effect [18]; a density threshold exists below which an initial population eventually gets extinct. Recent work on pattern formation in the presence of the Allee effect may be found in reference [13]. Finally, what we will call the *third type* of nonlinearity has $f(u)$ positive for $0 < u < 1$ but is nonlinear in u for small u. Reaction diffusion equations with these kinds of reaction terms have been used, for example, in studying thermal combustion waves [4,19], certain autocatalytic chemical reactions [20] and calcium deposition in bone formation [21]. In thermal combustion, nonlinear growth may represent the temperature profile [4] as well as the concentration of the reacting species [19], in chemical reactions, it represents the order of the autocatalysis [20], and in calcium deposition, the crystalline clusters that grow over the bulk of the bone proportionally to the square of its mass [21].

In the context of models of biological invasion, Allee effects have been studied extensively (see e.g. [22] and

[a] e-mail: lgiuggio@princeton.edu

references therein) since the early experimental works on the flour beetles of the genus *Tibolium* [23] or more recent ones on the *Aphis varians* [24] and whales [25]. In general, Allee effects are defined as strong or weak [26] depending on whether the per capita growth rate, $f(u)/u$, is, respectively, negative or positive at low densities. Here, the term weak refers to the fact that the population does not exhibit any threshold phenomena. It turns out, however, that little is mentioned in the literature about the possibility of a per capita growth rate equal to zero at zero densities, a case that should always apply by default to sexually reproducing individuals. Here we are interested in bridging the gap that exists in these studies.

If the reaction term is of the first type, as described above, it has been shown that there exists a minimum speed for the existence of traveling fronts [15,16]. Such fronts are termed *pulled fronts* due to their dynamics being dictated by the growth and spreading of the front tail [27–29]. The value of the asymptotic front speed can be simply obtained by calculating the spreading of small perturbations around the unstable state $u = 0$. For these nonlinearities, initial conditions whose fronts are sufficiently steep eventually settle into the traveling front shape with speed $2\sqrt{Daf'(0)}$. On the other hand, initial conditions with shallower initial profiles either reach a velocity larger than the minimal one or simply accelerate [29].

Fronts generated by reaction terms of the second type are called *bistable* since both $u = 1$ and $u = 0$ are linearly stable, whereas fronts from the third type of nonlinearity are generally termed *pushed* [30]. These *pushed fronts* derive their name from the fact that the dynamics in the nonlinear region of $f(u)$ drives the front propagation [28,29,31], 'pushing' the tail front forward. In such cases, linearization techniques applied to the reaction diffusion equation do not allow one to find the traveling front speed. The speed selection mechanism differs greatly between the pushed and the pulled regimes. The long-time convergence to the traveling front shape and speed is shown to be exponential in the former case [29,31] and algebraic in the latter [27,29].

Whereas a great deal of attention has been given in the reaction diffusion literature to the determination of the traveling wave front speed [14,32], the speed selection problem, i.e., the prediction of the asymptotic front speed from a given initial condition [33,34], and the long-time rate of convergence to that speed [29,35], the problem of the full transient dynamics has received little attention. Our interest is in making some contribution to the study of this problem. We ask how an initial condition evolves to the asymptotic traveling front shape and speed. We do so by analyzing the transient dynamics of reaction diffusion equations whose $f(u)$'s belong to the third type.

The paper is organized as follows: in Section 2 we select three specific forms of the nonlinearity and exhibit their resultant *analytically obtained* traveling wave front speed and shape. Section 3 is devoted to the study of their transient dynamics. Section 4 contains concluding remarks.

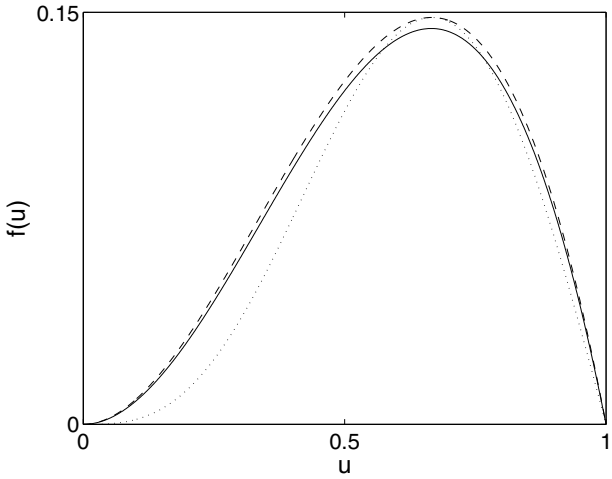

Fig. 1. Plot of the nonlinearities $f(u)$ under consideration. The solid and dashed curves represent $f(u)$ quadratic in u for small u as given, respectively, by equations (2) and (4). The dotted curve represents $f(u)$ given by equation (6) with $\eta = 16/(81\sqrt{3})$, an example of a nonlinearity cubic in u for small u.

2 Three specific nonlinearities and analytic traveling wave solutions

For some of the nonlinearities with $f'(0) = 0$ one can find exact analytic solutions for the traveling wave, making possible an exact description of both its shape and speed. We exploit the existence of these stable (see Appendix) pushed front solutions in studying the transient dynamics. We consider three examples of positive nonlinearity for $0 < u < 1$ with $f(u) \approx u^2$ as well as $f(u) \approx u^3$ for $u \approx 0$. These are depicted in Figure 1.

2.1 A logarithmic nonlinearity

Consider what we will henceforth call the *logarithmic* nonlinearity,

$$f(u) = (u+1)\left[2 - \ln(2) + \ln(u+1)\right] \ln^2(u+1)\left[\ln(2) - \ln(u+1)\right], \quad (2)$$

which is quadratic in u as $u \to 0$ and decreases linearly around $u = 1$. Despite its complicated appearance, we have managed to find exact analytic solutions of the traveling wave front and speed. The procedure requires the parametrization of the traveling front equation with $\partial u/\partial z$ instead of z (see e.g. Appendix C in Ref. [29] for the integration procedure). With the resulting differential equation solved exactly, an analytic value of the front speed can then be obtained. Integration of $(\partial u/\partial z)^{-1}$ and its inversion allows the determination of the exact traveling front profile. We have found the speed to be $c = \sqrt{Da}\ln(2)$ and its traveling front shape (centered around the origin) to have the analytic form, with $z = x - ct$,

$$u(z) = -1 + 2^{\left[1+\frac{\ln(4/3)}{\ln(3/2)}2^{z\sqrt{a/D}}\right]^{-1}}. \quad (3)$$

2.2 A special case of the ZF nonlinearity

Another example of a reaction term quadratic in u as $u \to 0$ may be obtained from the Zel'dovich–Frank-Kamenetsky equation by putting $b = 0$, i.e.,

$$f(u) = u^2(1-u). \tag{4}$$

The exact traveling wave front is given by

$$u(z) = \frac{1}{1 + e^{z\sqrt{a/2D}}}, \tag{5}$$

with $c = \sqrt{Da/2}$ as the front speed. In the following we call this $f(u)$ the *quadratic* nonlinearity.

2.3 A cubic nonlinearity

A nonlinearity which is cubic in u as $u \to 0$ can be obtained from a variety of systems including, e.g.,

$$f(u) = \eta \sin(\pi u)\left[1 - \cos(\pi u)\right]. \tag{6}$$

Given the periodicity of equation (6), we use it in our study only for initial conditions such that $u \leq 1$. The speed of the traveling front is given by $c = \sqrt{\eta\pi Da}$ and its traveling front shape is given

$$u(z) = \frac{2}{\pi}\arctan\left(e^{-z\sqrt{\eta\pi a/D}}\right). \tag{7}$$

The reaction term in equation (6) is a special case introduced to study the dynamics of the angle between the electric field and the polarization in ferroelectric chiral smectic liquid crystals [36]. For comparison purposes we choose $\eta = 16/(81\sqrt{3})$. This value of η ensures that equations (4) and (6) coincide at their peak $u = 2/3$. In the following we will call the *cubic* nonlinearity the $f(u)$ in equation (6) with η as given.

3 Transients during the formation of the traveling wave fronts

Our procedure for the study of transients consists of (i) assuming an initial condition roughly in the form of a 'right step' with $u = 1$ as $x \to -\infty$ and $u = 0$ as $x \to +\infty$, the form of the switchover being similar in shape, but not identical, to the eventual traveling front, (ii) computing a quantity that we call the *excess speed*, and (iii) studying the effects of various features of the initial conditions on the transient dynamics for the three types of nonlinearity considered. The excess speed is the amount by which the (eventual) traveling front speed c is exceeded by $v(t)$, the instantaneous time rate of change of the area under the front, i.e., $d\left[\int_{-\infty}^{+\infty} dx\, u(x,t)\right]/dt$, as explained, e.g., in reference [8]. It is a convenient quantity to focus on because it allows one to calculate how, overall, a front profile advances independently of how, on a local scale, the profile moves forward. Throughout this paper we have taken v to approach c if the differences is less than 10^{-8} in units of $\sqrt{Da}$.

Our numerical integration of the reaction diffusion equation is performed via an Adams-Bashforth-Moulton predictor corrector method with a spatial mesh of step size 0.08 in units of $\sqrt{D/a}$, which is the characteristic length of equation (1). We consider the front profile as separated into a *shoulder* for most of which $u = 1$, a *tail* which describes the final vanishing of u at long distances, and an in-between *interior* part. We construct our initial conditions by modifying the asymptotic traveling shape in these three parts separately or in combination. We report results mainly for tail-modified and interior-modified initial conditions since they are the ones that show the largest effects.

In Section 3.1 below, we first study initial conditions for the front obtained simply by replacing the characteristic length parameter $\sqrt{D/a}$ in the exact traveling front shape by a different value, the front shape being thus steeper or shallower than, but qualitatively identical to, the exact traveling front. In Sections 3.2 and 3.3, by contrast, we consider initial shapes that are different, even qualitatively, from the eventual traveling front shape. We obtain them by modifying, in the latter, only the interior portion in Section 3.2, and both the interior portion and the tail in Section 3.3.

3.1 Varying the characteristic length

The characteristic length $\sqrt{D/a}$ of the reaction diffusion system (1) appears naturally in the exact expressions (3), (5) and (7) for the traveling wave profile for the three nonlinearities, and controls the steepness of the front. In this subsection we investigate the transient occurring for initial conditions obtained by replacing $\sqrt{a/D}$ by $\xi^{-1}\sqrt{a/D}$ in the respective equations (3), (5) and (7). The quantity we vary is ξ, the dimensionless ratio of the length characteristic of the initial condition to $\sqrt{D/a}$. For values of ξ larger (smaller) than 1, the initial spatial profile is shallower (steeper) than the exact traveling front.

Our finding is that an initial condition constructed in this way gives rise to a monotonic decay of the front speed to the asymptotic value along with a change of the front steepness to the asymptotic shape. The long-time behavior appears exponential and can be fitted on a logarithmic scale by a straight line as exemplified in the inset of Figure 2. We calculate in this way the characteristic exponent of the decay for each of the three nonlinearities. We compare them in Figure 2 by plotting the decay time τ (reciprocal of the exponent) in units of $1/a$ as a function of the relative steepness ratio ξ. It is evident from Figure 2 that the decay time for the cubic nonlinearity is longer than that for the logarithmic nonlinearity. In turn, the logarithmic nonlinearity has a decay time longer than that for the quadratic nonlinearity. This hierarchy in time scales is due to the relative strength of the $f(u)$'s: the

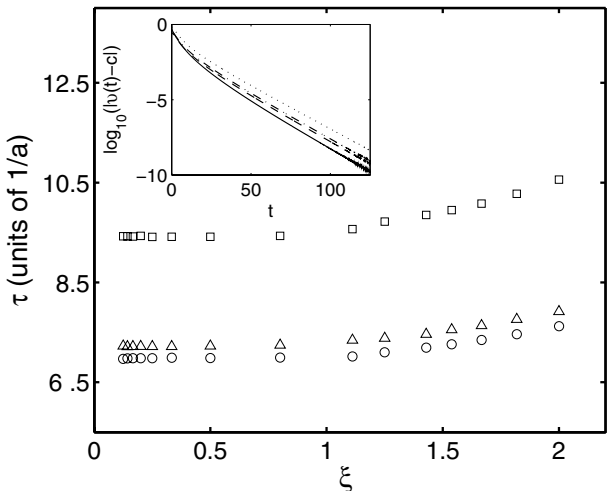

Fig. 2. Long-time decay constant τ of the initial front speed plotted in units of $1/a$ for the three nonlinearities depicted in Fig. 1. The horizontal axis is the dimensionless characteristic length ξ (see text). The triangles, the circles and the squares correspond, respectively, to the logarithmic, quadratic and cubic nonlinearity. If $\xi > 1$ (< 1), the initial front profile is shallower (steeper) than the asymptotic profile, and the front speed decreases (increases) monotonically to the asymptotic speed. The inset shows the evolution in time of the excess speed $v(t) - c$ on logarithmic scale for the quadratic nonlinearity. The solid, dashed, dash-dotted and dotted curves represent, respectively, an initial profile with $\xi = 0.250$, 1.429, 1.539, and 2.

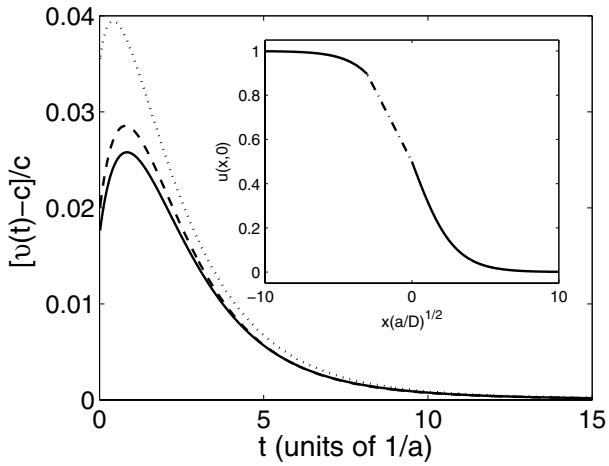

Fig. 3. Nonmonotonic behavior of the relative excess speed $[v(t) - c]/c$ as function of time. The solid, dashed and dotted curve represent the evolution of the relative excess speed for the logarithmic, quadratic and cubic nonlinearities, respectively. The initial condition is constructed as follows; it is a modification of the interior of the exact traveling front profile with a straight line segment depicted in the inset as dash-dotted. Only the initial condition for the logarithmic nonlinearity is shown in the inset since the three initial conditions are very similar to each other.

larger the value of the nonlinearity, the faster the rate of change of u. For a large portion of the interval $0 < u < 1$, the cubic nonlinearity has u values smaller than the other two. Similarly, the logarithmic nonlinearity has smaller values than the quadratic nonlinearity. The flat curve for $\xi < 1$ implies that an exponentially decaying front initially steeper than the traveling wave front approaches the asymptotic velocity independently of the specific shape at time $t = 0$. On the other hand, exponentially decaying fronts shallower than the asymptotic profile approaches the final velocity in a time that depends on the initial front shape: the shallower the longer the relaxation time. A qualitative similar dependence of the relaxation time on the initial condition has been reported by Van Saarloos (see Fig. 19 in Ref. [31]) in studying front propagation in what has been termed the nonlinear marginally stable regime.

3.2 Modification of the interior of the front: nonmonotonic behavior

Transients dynamics become more complex if the initial profile and the traveling front profile are qualitatively different. One example studied in this subsection is an initial profile obtained by modifying part of the interior of the exact traveling shape with a straight line segment. This segment starts at the coordinates $x = 0$, $u = 1/2$, and ends intersecting the exact traveling front profile at some point $x < 0$ (see the inset of Fig. 3). In other words, the initial profile is shallower than the asymptotic one in a limited region of space. Given that the portion of the asymptotic profile in the front interior modified to get the initial shape is rather small, one might expect a simple effect including a monotonic decay as in the previous section. Surprisingly, this does not happen. Rather than the distortion in the upper part of the interior disappearing, the shape in the lower part of the interior changes from the exact profile and becomes shallow first. During the transient dynamics, this situation corresponds to the appearance of a maximum in $v(t)$ as shown in Figure 3. At that instant, the evolution changes and $v(t)$ decays monotonically to the asymptotic value as shown in Figure 2. Notice that similar non-monotonic transients with the appearance of a maximum in $v(t)$ can be observed if the initial profile is taken as a modification of the exact profile for $x > 0$, e.g., with an exponential function that is shallower than the asymptotic front shape. In other words, if the lower, rather than the upper, part of the initial front interior is made shallower than the asymptotic shape, qualitatively similar dynamics are observed.

We define the ratio of the slope of the straight segment to the slope of the asymptotic traveling front at $u = 1/2$ as the relative steepness α. In Figure 4, we plot the time T_1 (in units $1/a$) at which the maximum of $v(t)$ appears as function of α. The inset shows the value H of the relative excess speed maximum as function of α. As α approaches 1, the distortion eventually becomes a small perturbation. The amplitude of this perturbation decays monotonically to the asymptotic profile, similarly to the long-time behavior described in Section 3.1. This explains why, for $\alpha \gtrsim 0.85$, the maximum disappears. Indeed, the

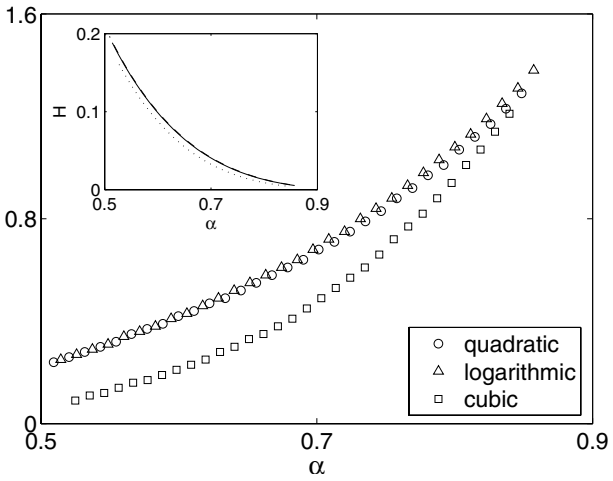

Fig. 4. Plot of T_1 the transient time for the appearance of the maximum in the relative excess speed as function of the relative steepness α of the initial conditions displayed in the inset of Figure 3. The inset shows the height H of the maximum of the relative excess speed as function of α.

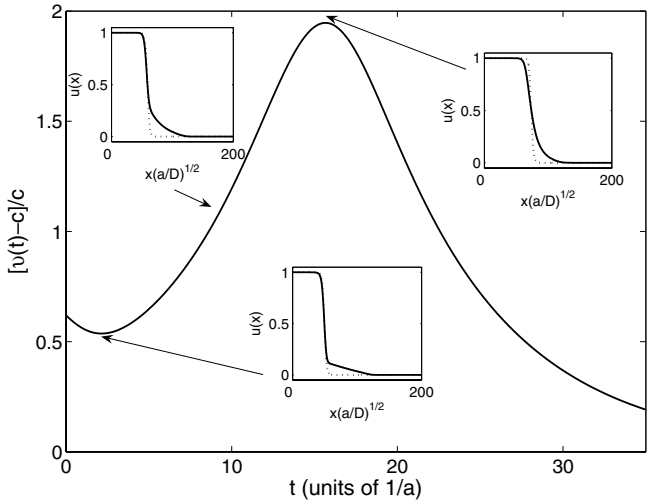

Fig. 5. Relative excess speed in the case of the nonlinearity given by equation (2) for an initial condition constructed as explained in the text. The various insets shows how the evolving front is different from the exact traveling front shape (dotted line) at different times. The exact traveling front is plotted by making the two curves cross each other at $u = 1/2$.

inset shows that the amplitude of the maximum becomes smaller as α increases. The other extreme corresponds to α approaching 0 when the initial profile tends to flatten out for $x < 0$. In such a case, the dynamics are dominated by the reaction term since the diffusion becomes negligible. It is a simple exercise to show that a flat profile for $u > 1/2$ approaches $u = 1$ exponentially fast. This explains why, for $\alpha \lessapprox 0.5$, the maximum in the relative excess speed also disappears.

3.3 Modification of both the tail and the interior

A common characteristic of the three nonlinearities we study is $f'(0) = 0$. This implies that the dynamics in the tail of the front are slower than the dynamics in the front interior. Therefore, we may expect an even more complex transient if the tail as well as the interior of the front are modified. We show our numerical results for this situation in Figure 5 for the logarithmic nonlinearity. The initial condition is chosen as follows. The lower part of the interior of the exact traveling front is cut off at an amplitude $A = 0.1$ by a straight line whose length depends on its steepness. This cut-off thus creates a tail which is infinitely steep. At the same time the rest of the front interior is modified from the shape of the exact solution by increasing the characteristic length $\sqrt{D/a}$ as in Section 3.1. In other words, the initial condition has an interior part which is shallower than the exact traveling front with its lower part modified with a straight line. Such an initial condition allows one to observe three different transient regimes. The first is associated with the time necessary for the interior part of the front to reduce its steepness and become essentially indistinguishable from the traveling front shape (see the center inset in Fig. 5). The second transient is created by the fast upwards propagation of the shallow straight line profile (see the top left inset in Fig. 5) present initially in the lower part of the front interior. These dynamics are similar to the one observed in Figures 3 and 4: eventually the interior front shape is converted into a shallow profile. When that happens once again $v(t)$ reaches a maximum. The final transient regime then corresponds to the monotonic decay to the asymptotic speed as shown earlier in Figure 2. Notice that, even though the initial front has a tail with compact support, i.e., is infinitely steep, that extreme steepness is not transferred to the front interior. On the contrary, it is the initial shallow upper interior that eventually makes the interior profile shallower than the traveling wave shape during the transient.

The appearance of the two extrema is also studied by selecting initial conditions whose interior parts have a given characteristic length larger than the asymptotic traveling front, and whose right-most portion is made up of a straight line segment proceeding from $u = A$ to $u = 0$. We keep the projection of the straight segment on the x-axis fixed and vary A. In the main part of Figure 6, we display four curves (solid, dotted, dashed and dash-dotted) with, respectively, increasingly larger values of A. The effect of the time scale disparity between the tail and front dynamics can be appreciated from Figure 6. At first, as A increases, the time lag between the minimum and maximum also increases. However, beyond a certain value of A, a larger portion of the shallow profile sees a rapidly increasing shape of the nonlinearity $f(u)$. The evolution of the initial front thus gets increasingly faster as A increases, reducing the time necessary for the profile to become shallow overall. This explains why the maximum of the dashed and dash-dotted curves move to the left. The inset of Figure 6 shows the variation of this time lag called T_2 as function of A for the three nonlinearities. This

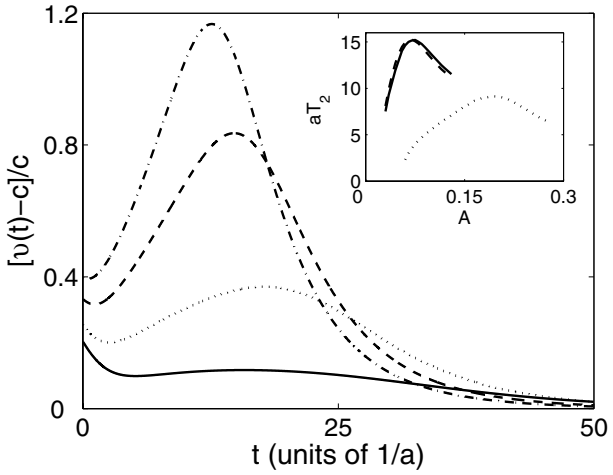

Fig. 6. Plot of the relative excess speed for the logarithmic nonlinearity as function of time for four initial fronts with different value of A (see text). The solid, dotted, dashed and dash-dotted curves correspond to $A = 0.04$, 0.06, 0.1 and 0.12, respectively. The inset shows how the delay time T_2 between the minimum and the maximum changes as function of A for the three nonlinearities.

transition is visible in all three cases but is more pronounced in the logarithmic and quadratic nonlinearities.

4 Concluding remarks

We have studied the transient dynamics of reaction diffusion systems whose reaction term $f(u)$ is characterized by being positive for $0 < u < 1$ with $f'(0) = 0$. Specifically, we have chosen two nonlinearities whose $f(u)$ is quadratic and one whose $f(u)$ is cubic for $u \approx 0$. We have found analytic expressions for the corresponding traveling front shape and speed. With the help of these expressions, we have analyzed how certain types of initial conditions evolve in time. Our initial conditions are simple modifications of the exact traveling front shape. Monotonic relaxation to the traveling front speed is observed if the initial front is qualitatively similar to the asymptotic profile, being constructed from the latter only by varying the characteristic length scale of the traveling wave front. Nonmonotonic behavior instead may be observed when the initial conditions are qualitatively different from the asymptotic profile. In such cases, the transient dynamics is dominated by the evolution of the interior part of the front since the tail evolution is much slower due to the nonlinear nature of $f(u)$ for $u \to 0$. The ensuing time scale disparity is responsible for the complicated observed time evolution of the front profile and front velocity. If part of the interior is shallower (steeper) than the asymptotic traveling front, the shallowness (steepness) is transferred to the whole interior profile, initially. Subsequently the velocity then decays monotonically to zero with the long time behavior being exponential.

Despite the complicated dynamics of the transient phenomena observed, the choice of relatively similar nonlinearities and sufficiently simple initial conditions have allowed us to identify the mechanisms responsible for the non-monotonic time dependence of the front traveling speed and its relation to the shape of $f(u)$. This analysis should allow one to obtain insights of the front dynamics in presence of more complicated initial conditions by identifying the relative steepness of the tail and front interior to the traveling wave front shape, as well as to cases of nonlinearities whose growth term increases with power exponent bigger than in those cases studied here.

The application of our results should have particular relevance in the context of species invasion where Allee effect, also called depensation [37], can dramatically impact the propagating speed of traveling fronts. By plotting the per capita growth rate $f(u)/u$ as function of u it is easy to see that the stronger the Allee effect the slower the propagating speed, lending support to the idea that depensation slows down the traveling wave fronts in reaction diffusion systems [26,39].

Transient dynamics in reaction diffusion systems is rarely studied, mostly due to the difficulty of the problem. In this work, by comparing three different reaction terms, and by using sufficiently simple initial conditions, we have been able to understand part of the front dynamics and in particular its non-monotonic time dependence. A theoretical analysis such as ours becomes crucially important when the front does not reach the asymptotic traveling regime. In such cases the concept of a traveling front speed and shape cannot be applied to experimental observations and an understanding of the dynamics becomes necessary. We hope that our study will motivate further research on the formation of the traveling front profile in reaction diffusion systems.

This work was supported in part by the NSF under grant no. INT-0336343, by NSF/NIH Ecology of Infectious Diseases under grant no. EF-0326757, by the Program in Interdisciplinary Biological and Biomedical Sciences at UNM funded by the Howard Hughes Medical Institute, and by DARPA under grant no. DARPA-N00014-03-1-0900.

Appendix

In the first part of this section we study the linear stability of our traveling fronts to perturbation, and in the second part we study the structural stability of the corresponding reaction diffusion equations.

In order to study the stability of the traveling wave fronts to perturbations, we follow the standard procedure [7,29,30]. We take the normalized version of equation (1)

$$\frac{\partial u(y,\tau)}{\partial \tau} = \frac{\partial^2 u(y,\tau)}{\partial y^2} + f(u(y,\tau)). \tag{8}$$

where y and τ are dimensionless variables and we consider the perturbation $v(\varsigma,\tau)$ where $\varsigma = y - \omega\tau$ with ω the dimensionless travelling speed. We look at the evolution

of $v(\varsigma,\tau)$ when such perturbation is small, i.e., we take the perturbed traveling wave front

$$u(\varsigma,\tau) = u_0^\omega(\varsigma) + \epsilon v(\varsigma,\tau), \tag{9}$$

where $\epsilon \ll 1$ and where $u_0^\omega(\varsigma)$ is the traveling wave solution. We insert equation (9) into equation (8) and Taylor expand the nonlinearity $f(u_0^\omega(z)+\epsilon v(\varsigma,t))$ only up to first order in ϵ. After some algebra and by assuming, for convenience, $v(\varsigma,\tau) = \xi(\varsigma)e^{-\omega\varsigma/2}e^{-\lambda\tau}$, the equation satisfying $\xi(\varsigma)$ is given by

$$-\frac{d^2\xi(\varsigma)}{d\varsigma^2} + \left(\frac{\omega^2}{4} - f'(u_0^\omega(\varsigma))\right)\xi(\varsigma) = \lambda\xi(\varsigma), \tag{10}$$

where $\xi(\varsigma)$ decays to zero for large $|\varsigma|$ in such a way that $\lim_{\varsigma\to\pm\infty}\xi(\varsigma)e^{-\omega\varsigma/2} = 0$. By defining the operator $H = \left[-\frac{d^2}{d\varsigma^2} + \frac{\omega^2}{4} - f'(u_0^\omega(\varsigma))\right]$, equation (10) can be cast into the form

$$H\xi_\lambda = \lambda\xi_\lambda. \tag{11}$$

The determination of the coefficient λ becomes formally equivalent to the calculation of the eigenvalues of a time independent Schrödinger equation with a potential energy $V(\varsigma) = \omega^2/4 - f'(u_0^\omega(\varsigma))$ and with ξ_λ the corresponding eigenfunctions. We now find the eigenfunctions of H that corresponds to $\lambda = 0$ and argue that it is the lowest eigenvalue of H. We point out that the eigenvalue $\lambda = 0$ corresponds to a translated traveling wave since the perturbation does not grow and neither decays [7,30]. Expanding to first order in ϵ the translated traveling wave $u_0^\omega(\varsigma+\epsilon)$ we can identify

$$\xi_0(z) = e^{\omega\varsigma/2}\frac{du_0^\omega(\varsigma)}{d\varsigma}. \tag{12}$$

Since the front shapes are monotonically decreasing functions of ς, $du_0^\omega(\varsigma)/d\varsigma$ is always negative. This means that $\xi_0(\varsigma)$ does not have any roots and the *wave function* corresponding to $\lambda = 0$ is nodeless. It is well known in quantum mechanics that [41] the nodeless wave function would correspond to the ground state of the system with lowest λ. This implies that all the other eigenvalues are larger than zero. The traveling fronts in equations (2), (4) and (6) are thus stable to small perturbations in the moving frame. An initial condition, which is constructed by infinitesimally modifying the traveling front profile, will converge to the asymptotic shape and attain the traveling front speed.

The structural stability analysis allows one to determine if the traveling front solutions suffer only infinitesimal change when the nonlinearity $f(u)$ is perturbed infinitesimally to $\delta f(u)$. We are concerned here with two types of modifications of $f(u)$. A quantitative variation of the growth term and a qualitative variation of the growth term. For this purpose we follow in part the renormalization procedure detailed in reference [38] that allows one to calculate the variation of the traveling speed $\delta\omega$ from the perturbation $\delta f(u)$ (see Eq. (9) in Ref. [38]). If $\delta f(u) = \epsilon f(u)$, we find that $\delta\omega \approx 0.34\epsilon$, $\delta\omega = 2^{-3/2}\epsilon$, and $\delta\omega = 2\pi^{1/2}3^{-9/4}\epsilon$ for the logarithmic, the quadratic and the cubic nonlinearity, respectively. For a qualitative modification of the form of $f(u)$ we are interested in modifications where the power exponent close to $u = 0$ becomes larger than in the original $f(u)$. We consider the extreme situation where the power becomes infinitely large and the growth term becomes flat, so as to include situations when the exponent variation is smaller. We choose $\delta f(u) = \Theta(u-\epsilon)f(u)$ where Θ represents the Heaviside step function. For calculating the variation $\delta\omega$ in this case, it is more convenient to simply construct the traveling front for the modified nonlinearity by joining together the exact solution for $u > \epsilon$ and the one when $u < \epsilon$ [40] with the result

$$\begin{aligned}
\delta\omega &= -\ln(2) + \frac{[\ln(2) - \ln(1+\epsilon)]\ln(1+\epsilon)}{\epsilon},\\
\delta\omega &= -\frac{\epsilon}{\sqrt{2}},\\
\delta\omega &= \sqrt{\pi\eta}\left[\frac{\sin(\pi\epsilon)}{\pi\epsilon} - 1\right],
\end{aligned} \tag{13}$$

for, respectively, the logarithmic, quadratic and cubic nonlinearity. Notice that $\delta\omega \to 0^-$ as $\epsilon \to 0^+$, proportional to ϵ in the first two cases and proportional to ϵ^3 for the cubic nonlinearity. We thus have shown that infinitesimal quantitative as well as qualitative modification in the growth term of $f(u)$ change the traveling front solution only infinitesimally, pointing to the structural stability of the equations we have analyzed.

References

1. G. Parisi, Y.C. Zhang, J. Stat. Phys. **41**, 1 (1985)
2. D. Bensimon, B. Shraiman, L.P. Kadanoff, in *Kinetics of Aggregation and Gelation*, edited by F. Family, D.P. Landau (Elsevier-North Holland, Amsterdam, 1984)
3. P. Gray, S.K. Scott, *Chemical Oscillations and Instabilities: non-linear chemical kinetics* (Oxford Univ. Press, 1994)
4. Ya.B. Zel'dovich, G.I. Barenblatt, Combust. Flame **3**, 61 (1959)
5. A.C. Scott, Rev. Mod. Phys. **47**, 487 (1975); A.C. Scott, *Neurophysics* (Wiley, New York, 1977)
6. A. Okubo, S. Levin, *Diffusion and Ecological Problems: Modern Perspectives*, 2nd edn. (Springer-Verlag, Berlin, 2001)
7. J.D. Murray, *Mathematical Biology*, 2nd edn. (Springer, New York, 1993)
8. L. Giuggioli, V.M. Kenkre, Physica D **183**, 245 (2004)
9. I.D. Peixoto, L. Giuggioli, V.M. Kenkre, Phys. Rev. E **72**, 041902 (2005)
10. K.K. Manne, A.J. Hurd, V.M. Kenkre, Phys. Rev. E **61**, 4177 (2000)
11. G. Abramson, A.R. Bishop, V.M. Kenkre, Phys. Rev. E **64**, 66615 (2001)
12. M.A. Fuentes, M.N. Kuperman, V.M. Kenkre, Phys. Rev. Lett. **91**, 158104 (2003); J. Phys. Chem. B **108**, 10505 (2004)

13. M.G. Clerc, D. Escaff, V.M. Kenkre, Phs. Rev. E **72**, 056217 (2005)
14. R.D. Benguria, M.C. Depassier, Phys. Rev. Lett. **77**, 1171 (1996); Phys. Rev. E **75**, 51106 (2007)
15. R.A. Fisher, Ann. Eugen. **7**, 355 (1937)
16. A. Kolmogorov, I. Petrovsky, N. Piskunov, Bull. Univ. Moskou, Ser. Internat., Sec. A **1**, 1 (1937)
17. Ya.B. Zel'dovich, D.A. Frank-Kamenetsky, Doklady Akademii Nauk. SSSR, **19**, 693 (1938)
18. W.C. Allee, *The Social Life of Animals* (Beacon Press, Boston, MA, USA, 1938)
19. P. Calvin, Ann. Rev. Fluid Mech. **26**, 321 (1994)
20. M.J. Metcalf, J.H. Merkin, S.K. Scott, Proc. R. Soc. Lond. A **447**, 155 (1994)
21. P. Tracqui, A.M. Perault-Staub, G. Milhaud, J.F. Staub, Bull. Math. Biol. **49**, 597 (1987)
22. M.-H. Wang, M. Kot, M.G. Neubert, J. Math. Biol. **44**, 150 (2002)
23. R.N. Chapman, Ecology **9**, 11 (1928)
24. P. Truchin, P. Kareiva, Ecology **70**, 1008 (1989)
25. C.W. Fowler, J.D. Baker, Rep. Int. Whal. Commn. **41**, 545 (1991)
26. M.-H. Wang, M. Kot, Math. Biosciences **171**, 83 (2001)
27. W. van Saarloos, Phys. Rev. A **37**, 211 (1988)
28. U. Ebert, W. van Saarloos, Phys. Rev. Lett. **80**, 1650 (1998)
29. U. Ebert, W. van Saarloos, Physica D **146**, 1 (2000)
30. D. Panja, W. van Saarloos, Phys. Rev. E **65**, 057202 (2002)
31. W. van Saarloos, Phys. Rev. A **39**, 6367 (1989)
32. R.D. Benguria, M.C. Depassier, Phys. Rev. E **50**, 3701 (1994) and references therein
33. D.G. Aronson, H.F. Weinberger, Adv. Math. **30**, 33 (1978)
34. M. Bransom, Mem. Am. Math. Soc. **285**, 1 (1983)
35. W. van Saarloos, Phys. Rev. A Phys. Rep. **386**, 29 (2003)
36. W. van Saarloos, M. van Hecke, R. Holyst, Phys. Rev. E **52**, 1773 (1995)
37. C.W. Clark in *Mathematical bioeconomics: the optimal management of renewable resource* (Wiley, New York, 1990)
38. G.C. Paquette, L.-Y. Chen, N. Goldenfeld, Y. Oono, Phys. Rev. Lett. **72**, 76 (1994)
39. M.A. Lewis, P. Kareiva, Theor. Pop. Biol. **43**, 141 (1993)
40. E. Brunet, B. Derrida, Phys. Rev. E **56**, 2597 (1997)
41. P. Morse, H. Feshbach, *Methods of Theoretical Physics Part I* (McGraw Hill 1953), Chap. 5, Sect. 2